16th ICAAR LISBOA 2020-2022

16th International Conference on
Alkali-Aggregate Reaction in Concrete
Lisboa | LNEC | Portugal | 31 May - 2 June 2022

http://icaar2020-2022.lnec.pt

Mitigation of AAR structural effects by creep of concrete: experiments and modelling

Clement Lacombe [(1)], Alain Sellier [(2)], Thierry Vidal [(3)], Christine Noret [(4)], Patrice Anthiniac [(5)]

(1) LMDC / TRACTEBEL Engineering Fr, Toulouse, France, clement.lacombe@tractebel.engie.fr

(2) LMDC, Toulouse, France, alain.sellier@insa-toulouse.fr

(3) LMDC, Toulouse, France, thierry.vidal@univ-tlse3.fr

(4) TRACTEBEL Engineering Fr, Gennevilliers, France, christine.noret@tractebel.engie.com

(5) TRACTEBEL Engineering Fr, Toulouse, France, patrice.anthiniac@tractebel.engie.com

Abstract

In the current context of growing demand for green energy and environment protection, the durability of former hydropower dams is an important issue. Some concrete dams are affected by Alkali Aggregate Reaction (AAR), which may give rise to major concern for their safety. In the case of an arch dam, the AAR swelling of concrete can induce higher stresses and a major change in the stress distribution within the structure and its abutment. The observable symptoms are generally irreversible displacements of the dam crest in the upstream direction. As concrete creeps under mechanical loading, the stress level evolves with the creep potential of the concrete, which could, itself, be modified by AAR. In the laboratory, swelling under imposed stress has been studied in previous research but the creep velocity of concrete damaged by free AAR remains poorly known. So, we present here an original experimental programme where the concrete behaviour is studied through this creep and the simultaneous AAR configuration. Two concrete mixes are studied: one with reactive aggregates and the other with non-reactive aggregates. The mixes were similar regarding the proportions of cement, water, sand and aggregates so as to obtain similar mechanical properties before AAR and, thus, to focus the comparative creep analysis on the effects of AAR only. All the specimens were maintained in autogenous conditions for 28 days before being immersed in1M sodium hydroxide solution at 38°C (100°F) to initiate the AAR. Once a swelling of 0.04% had been reached, the specimens were taken out of the solution and immediately protected from desiccation to keep water available in the porosity for further evolution of the AAR. Half of the specimens were placed under sustained uniaxial compressive loading while the others were free to deform. Results from this programme were used to fit and validate a new non-linear homogenization method coupling creep and swelling mechanisms. This new type of model, when implemented in a finite element code, should allow the ageing of AAR affected dams to be better represented.

***Keywords**: alkali-aggregate reaction; creep; arch dam*

1. INTRODUCTION

Studies of the Alkali-Aggregate Reaction (AAR) and its structural consequences began upon its discovery in the 1940s. After identification of the main causes [1] of the reaction, namely alkali-sensitive aggregates, and high relative humidity and alkali content in the cement, the scientific community turned its attention to the effects of AAR on the mechanical properties of concrete and their evolution under various types of loading.

In 1997, Larive [2] proposed an exponential law to describe the free swelling induced by the reaction. However, if the reactive concrete specimens are loaded before the reaction initiation [3], these free strains can be reduced or cancelled in the stress directions. In 1994, Charlwood [4], established a first logarithmic relationship between the swelling rate and the applied stresses, in which swelling totally vanished under 8 MPa compression. This model was the first of a long series reviewed in 2017 [5].

Some of these models consider such swelling reduction by coupling creep and AAR at the concrete scale [6] or try to explain it using micro-mechanical modelling [7]. In these models, one explanation involves creep of the cement paste just around the aggregates at a velocity sufficient to absorb the gel

overpressure. This is a kind of absorption of the swelling by the viscoelastic behaviour of the cement matrix. If this point is to be taken into consideration for future models, the first step is to quantify it.

In the case of arch dams, the swelling induced by the AAR can change the stress distribution and may lead to higher stresses. So, it is essential to study the reaction and its effects on delayed strain under late loading. In 2019, Reinhardt et al. [8] began work on the time-dependent strains of concretes incorporating different types of aggregates at different rates of expansion. They quantified these strains but the reaction had already stopped when the load was applied. The creep of an AAR-affected concrete that is initially free to swell but is loaded before the end of the reaction has never been measured. The experimental programme presented here concerns this configuration and its main objective is to clarify the interactions between the creep behaviour and the ongoing AAR.

2. EXPERIMENTAL TEST PROGRAMME

2.1 General

The observation of AAR structural effects by creep of concrete requires the study of two concretes, one reactive and the other not, stored and loaded in the same conditions. These two concrete mixes should be designed to reach similar mechanical properties so that the observed difference of delayed behaviour can be interpreted as a consequence of the AAR. Experimentation with unloaded specimens is also needed to quantify the free swelling of the concrete due to the AAR.

2.2 Choice of aggregates

Keeping in mind that the two concrete mixes had to be similar before the AAR development, the aggregates chosen had initial mechanical properties and granular distributions that were close. Crushed limestone aggregate was chosen for the non-reactive mix and crushed calcareous-siliceous aggregate for the reactive one, the latter being classified as PR (potentially reactive) according to the LCPC classification [9]. Crushed limestone aggregates have already been studied by Makani [10], so their mechanical properties are known and are presented in Table 2.1. The reactive aggregate was characterized in accordance with standards [11] [12] and the results are also presented in Table 2.1 for comparison. The 58 mm diameter specimens were extracted from a 25 cm cube of boulder rock, and the cores were then sawn to obtain a slenderness of 2:1.

Table 2.1. Mechanical properties of the source of the aggregates

Name of rock	Non-reactive [10]	Reactive
Uniaxial compressive strength	224 ± 25 MPa	178 ± 47 MPa
Young's modulus	80 ± 2 GPa	78.6 ± 0.2 GPa
Poisson's ratio	0.31± 0.01	0.31 ± 0.02

2.3 Concrete composition

The two concrete mixes were similar regarding the proportions of materials, with 1713 kg/m^3 of aggregates, 410 kg/m^3 of cement, and a water/cement ratio of 0.46. The two aggregate grading curves were fitted on the same granular distributions but the sand/grain ratio was slightly different because of the grading curve of each kind of aggregate. To minimize this effect, the maximum size was crushed so that 100% passed through the 12.5 mm sieve for both. The detailed compositions of the mixes are presented in Table 2.2. The cement used for both mixes was a CEM I 52.5 R, in which the equivalent Na_2O had been increased from 0.28% to 1.25% by adding sodium hydroxide in the mixing water to be sure that the reaction had enough alkali for its development.

Table 2.2. Concrete compositions

Mix name		Non-reactive	Reactive
Components			
Sand	NON-REACTIVE 0-2	680 kg/m^3	/
	REACTIVE 0-4	/	672 kg/m^3
Aggregate	NON-REACTIVE 4-12.5	1041 kg/m^3	/
	REACTIVE 4-6	/	190 kg/m^3
	REACTIVE 6-12.5	/	843 kg/m^3
Cement		410 kg/m^3	
Water/cement ratio		0.46	

2.4 Chronology of exposure and loading conditions

The test programme consisted of three stages. From one day after mixing to 28 days, the specimens were stored in autogenous conditions at 20°C. In the second stage, they were immersed in a 1M hydroxide solution kept in barrels, themselves stored at 38°C to accelerate the reaction. This concentration was chosen in accordance with the results of previous experiments [13] to avoid the leaching of alkalis. Once a swelling of 0.04% was reached, all the concrete specimens were protected from desiccation. Following this stage, half the specimens of each mix (reactive and non-reactive) were placed under uniaxial compressive loading corresponding to 30 % of the lowest compressive strength observed in either of the concrete compositions. The other samples remained free to deform at 20°C. At the end date of each stage, the compressive strength and the Young's modulus of the two mixes were assessed in accordance with standards [11] [12].

2.5 Specimens and measurements

For each concrete, 11 samples were cast: 6 were used for the mechanical characterization (3 at 2 specific dates), 3 for the free strain measurements, and 2 for the creep test. The samples were cylinders 11.3 cm in diameter and 22 cm in height (slenderness of 2:1). The free strains were measured on specimens instrumented with stainless steel shrinkage plugs.

This measurement system complied with the norm [14]. The references for strains were taken just after demoulding on day 1. During the 38°C heating period, the measurements were made weekly after one day of cooling from 38°C to 20°C. The strains of specimens under loading were recorded from the displacement measurements of an inner LVDT sensor located in a niche in the central part of the cylinders for creep tests, which also permitted the shrinkage to be measured during curing. For creep tests, the uniaxial compression load was applied through the hydraulic jack of the creep setup, using a hydraulic pump. The creep tests were performed in a room at 20°C.

3. RESULTS AND DISCUSSION

3.1 Designations and curve conventions

All the results are presented with the same nomenclature. The non-reactive concrete samples are named NR and are presented in blue, the reactive specimens are named R and they are in red. The letter following the reactivity indication specifies the kind of measurement system: IS for the inner sensor and P for the plugs. The results given by these two systems are represented by continuous lines and dashed lines, respectively. In all the figures, shrinkage and creep are negative, while swelling is positive.

3.2 Autogenous shrinkage during curing

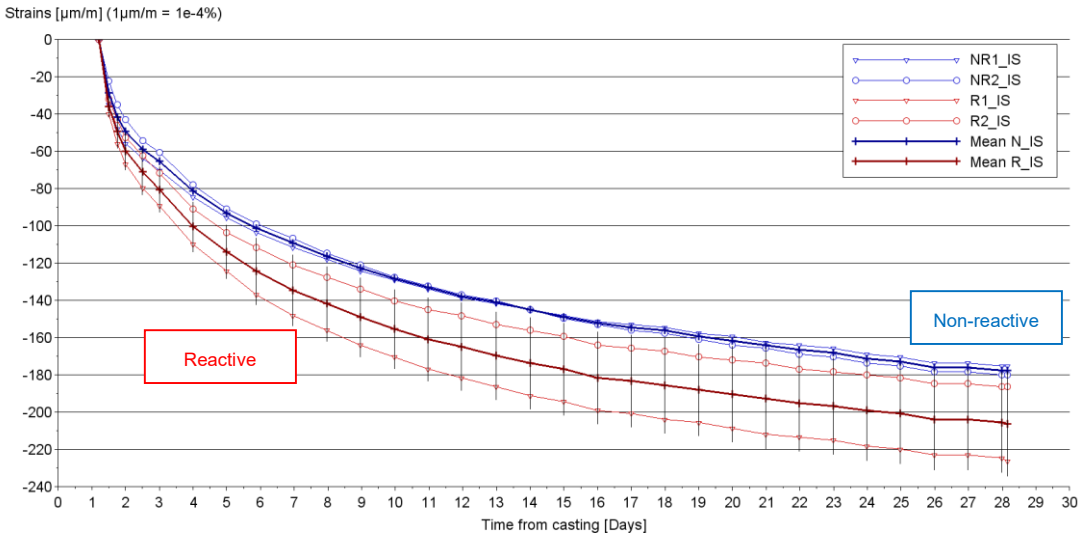

Figure 3.1. Autogenous shrinkage strains for reactive and non-reactive specimens during the 20°C autogenous curing (measurement by inner sensor)

The autogenous shrinkage during the 28 days of curing are presented in Figure 3.1. At the end of this experimental phase, the mean shrinkage strains measured by inner sensors were 178 ± 3 µm/m and 206 ± 28 µm/m for the non-reactive and reactive concretes, respectively. The measurements on the plug specimens at 28 days were 124 ± 13 µm/m for the non-reactive specimens and 137 ± 5 µm/m for the reactive ones.

It can be assumed that the difference between all the measurements could be a consequence of the high shrinkage rate at very early age. The times of initial measurements of the specimens could be slightly different, inducing a slight lag in the measured evolution. Moreover, a short drying period could occur during the placement of sensors and plugs and may have been different for each specimen. If these causes of discrepancy and the evolutions after the first five days are considered, the shrinkages of the two concrete types are quite similar.

Note that the values of autogenous shrinkage are higher than those of concrete compositions with normal alkali content and the same water/cement ratio. This may be a result of the higher alkali content [15].

3.3 AAR Expansions and free strains

The AAR expansions and strains due to water absorption and shrinkage, after the 28-day curing period, are presented in Figure 3.2. The analyses of these evolutions are divided into two parts. The first deals with the swelling in solution and at 38°C, while the second concerns the free strains in autogenous conditions at 20°C.

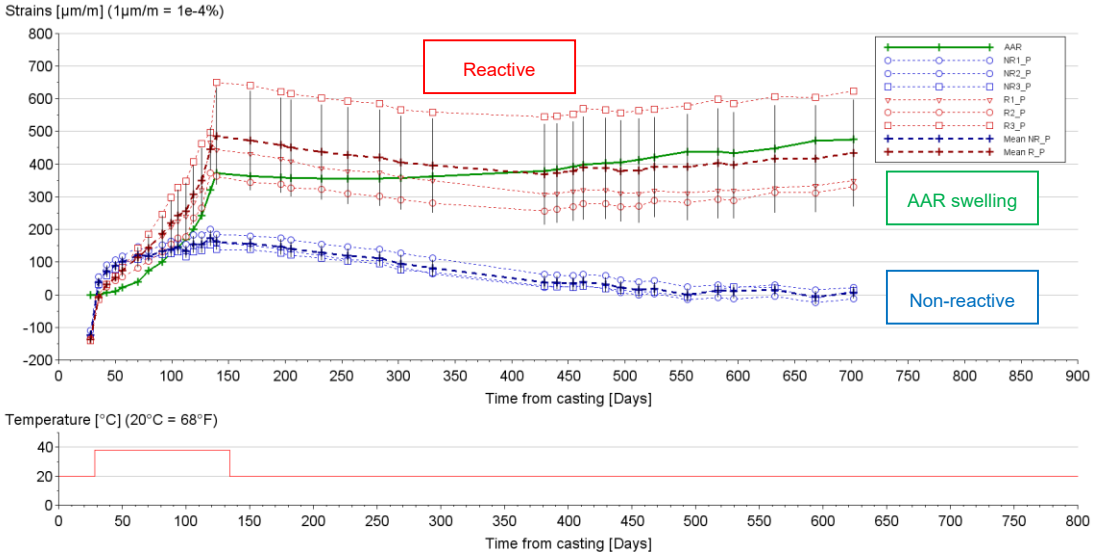

Figure 3.2. Evolution of free strains of the reactive (red) and non-reactive (blue) specimens from 28 days to 700 days. The green line corresponds to the difference between reactive and non-reactive concrete strain evolutions

3.3.1 Evolution under NaOH solution at 38°C

The AAR evolution corresponds to the difference between the strain evolutions of the reactive composition and the non-reactive one (green line in Figure 3.2). The initial value to quantify swelling was taken one week after immersion in water in order to subtract the strains due to water absorption. After 30 days in solution, the mass variations are identical but a swelling appears on the reactive specimens. At the end of the accelerated reaction, the reactive and non-reactive specimens reach swellings of 446 ± 64 and 173 ± 24 µm/m, respectively, corresponding to an AAR swelling of 0.032%.

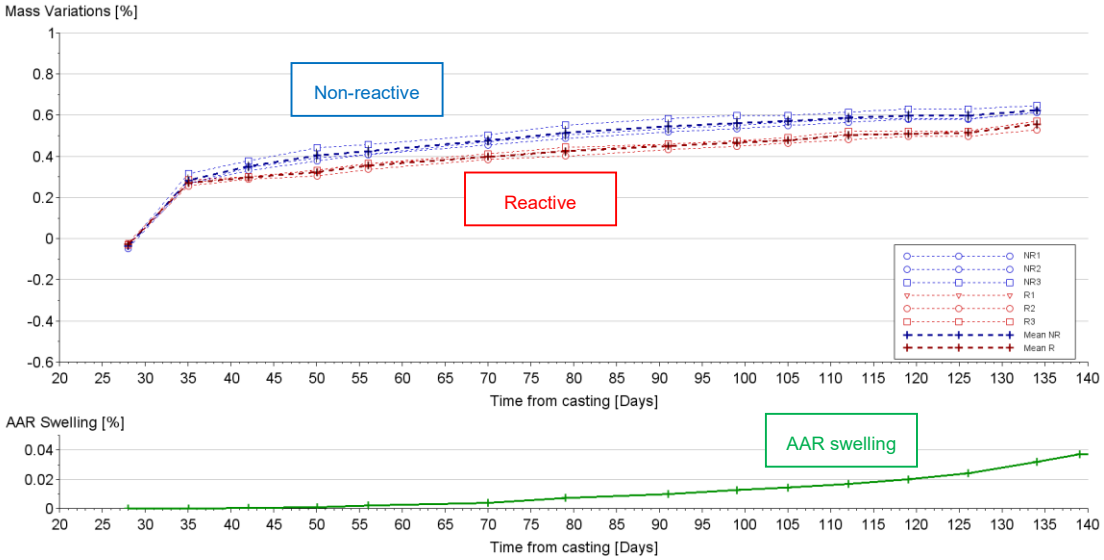

Figure 3.3. Mass variation of the specimens during the immersion in NaOH solution at 38°C and the AAR swelling evolution during the same period

3.3.2 Free strains under autogenous conditions

Strain measurements were recorded just before and after the operation to seal the specimens in autogenous conditions. In autogenous conditions at 20°C, the AAR continues and evolves from 0.032% to 0.037%. In Figure 3.4, the swelling curve shows slight shrinkage in the first phase under these conditions, followed by slow swelling.

The reduction in swelling rate can be attributed, on the one hand, to the temperature decreasing from 38°C to 20°C (already observed in [16] [2]) and, on the other, to alkali diffusion from cement paste to reactive aggregates becoming more difficult due to the change of moisture conditions (alkaline water bath to autogenous conditions), which can cause some unexpected drying shrinkage. However, after one year, the reaction becomes faster than the shrinkage and the swelling curve restarts. This evolution is in agreement with the theory that the autogenous condition following a wet stage significantly reduces the swelling rate but is still sufficient to allow the reaction to continue [17].

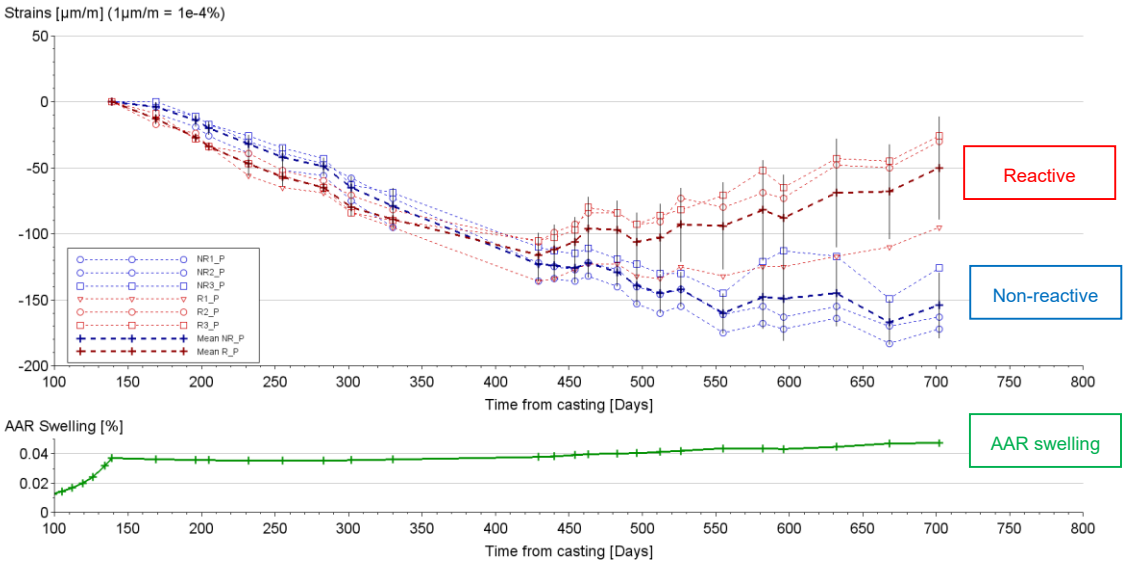

Figure 3.4 Top: Evolution of free strains for a reset at the beginning of the autogenous stage, bottom, AAR free swelling from 100 days after casting

3.4 Evolution of mechanical properties

The mechanical properties of both concrete mixes were tested at two concrete ages, before immersion and at the end of the immersion stage. The results are presented in Table 3.1.

Table 3.1. Mechanical properties before and after immersion time

Composition	Non-reactive	Reactive	Relative difference [%]
Compressive Strength			
35 days	45.3 ± 1.2 MPa	51.1 ± 0.6 MPa	+ 12.8 %
136 days	56.2 ± 1.0 MPa	59.2 ± 0.9 MPa	- 4.70 %
Evolution	+ 24.8 %	+ 15.8 %	/
Young's modulus			
35 days	39.2 ± 0.6 GPa	37.3 ± 0.4 GPa	- 4.79 %
136 days	41.7 ± 0.2GPa	36.1 ± 0.4 GPa	- 13.4 %
Evolution	+ 6.39 %	- 3.25 %	/

The mechanical tests were performed at 35 days on specimens stored in autogenous conditions. The aim of this first characterization was to compare the mechanical performances of the concretes before swelling. The Young's modulus of the reactive composition was 5% lower than for the non-reactive composition. This result can be explained by the fact that the Young's modulus was smaller for the reactive than the non-reactive aggregate (cf. Table 2.1). After 0.032% AAR swelling, the Young's modulus of the concrete affected by AAR decreased by 3.25% while that of the non-reactive one rose by 6.39%. The Young's modulus reduction during AAR is in line with previous observations [2] [8] and is the consequence of micro-cracking in the cement paste.

Nevertheless, the compressive strength of the reactive samples, rather than decreasing, increased by 14.8%. This evolution should be compared to the evolution of the non-reactive concrete, where the increase was 24.8%. So, it can be assumed than the AAR also affects the compressive strength but without neutralizing the benefits of hydration [2].

3.5 Time-dependent strains under a uniaxial load

3.5.1 Loading and elastic strains

Specimens were loaded uniaxially with the same compression stresses of 17 MPa, corresponding to 30% of the compressive strength measured on the non-reactive specimens at the age of loading (135 days, cf. Table 3.1). During loading, the Young's modulus was assessed for the two concretes. Their values were both 18% higher than the values presented in Table 3.1 and prove that the specimens had properties similar to those noted in the table.

The elastic strains measured for a 17 MPa compressive stress were 243 and 228 µm/m for the reactive and non-reactive compositions respectively. So, the strains of the reactive composition were 7% higher than those of the non-reactive one.

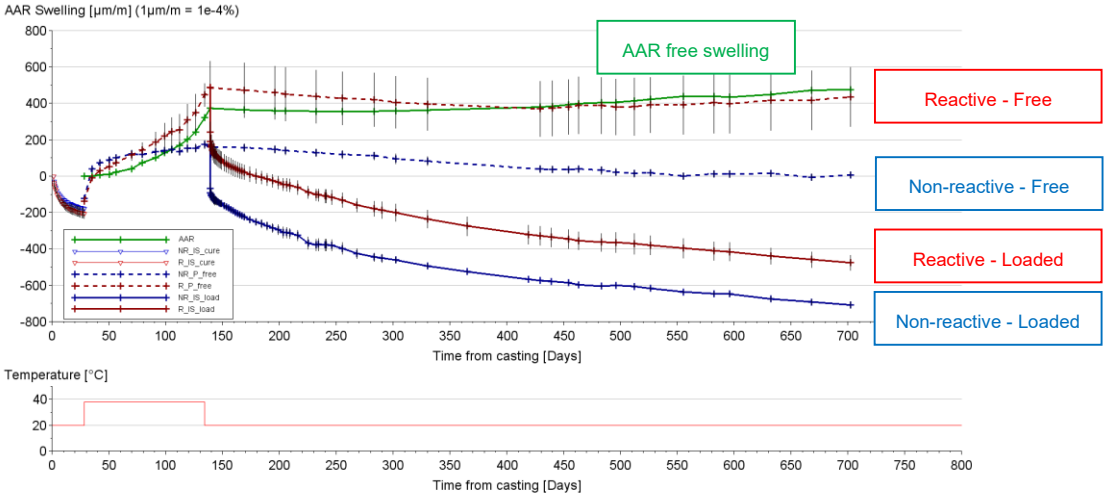

Figure 3.5. Total axial strains for all the test conditions

3.5.2 Strains under loading

The strains measured by inner sensors during the creep test are presented in Figure 3.5, and Figure 3.6 presents the evolutions of total strains during the creep tests.

The strains under loading (swelling and loading) remained higher for the reactive than the non-reactive concrete even after 700 days. At this date, the difference was 232 µm/m, so the loading reduced the AAR free swelling by 25%. This swelling reduction was due both to an instantaneous strain higher than for the NR specimens and to faster creep of R specimens during the first 15 days after loading. After this stage, the creep rates of the two concretes were very similar despite the low AAR observed in free swelling during the same period.

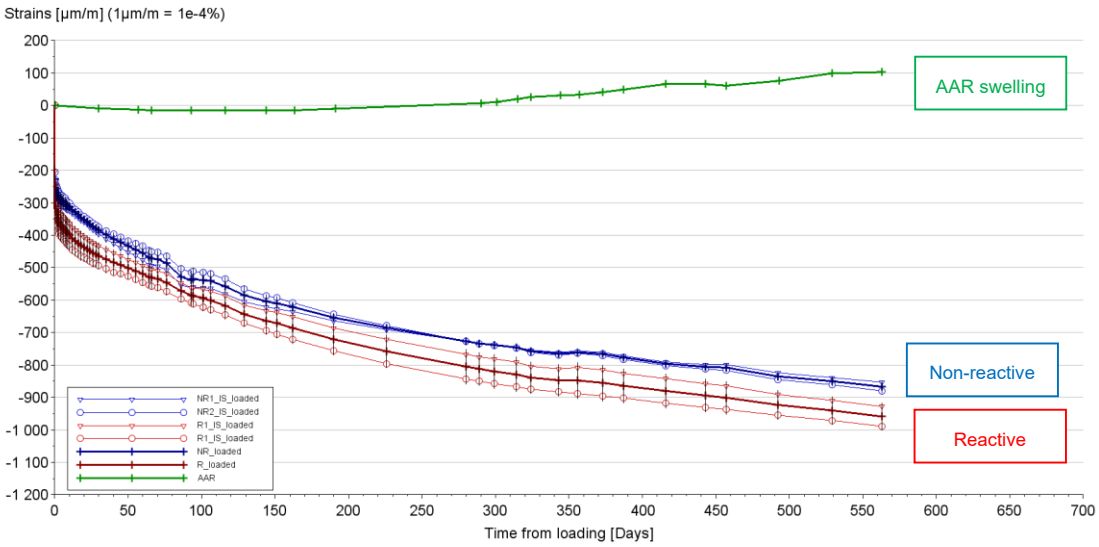

Figure 3.5 : Strains under load and AAR swelling during loading time

These results agree with the observations of Reinhardt et al. [8] where, after two weeks under stress, the creep velocities were very similar whatever the AAR advancement. In their study, the reaction had already stopped when the specimens were loaded for the creep tests. In our tests, despite the continuation of AAR, a swelling reduction of 25% could also be observed under a stress corresponding to 30% of the concrete compressive strength, without effects on the creep velocity during the end of the test. These results show that AAR swelling is partially reversible under compressive stress, and the role of creep in this swelling reduction is around 30%, mainly in the short term (a few days).

4. CONCLUSIONS AND MODELLING PROSPECTS

The comparative study of a reactive and a non-reactive concrete with very similar initial mechanical performances has allowed us to quantify the effects of creep occurring after a first stage of free swelling. The AAR swelling previous to the creep test can be reduced by 25% through application of a compressive stress corresponding to 30% of the concrete compressive strength. The creep rate is only affected during the first 10 days of loading and contributes to about 10% of this reduction, while the elastic behaviour absorbs 20% of the previous swelling. After this recovery stage, the creep rate is the same as for a non-reactive concrete despite the continuation of the AAR. This behaviour must be taken into consideration for modelling. In order to include these observed effects in a structural model, a micromechanics-based formulation is under development at LMDC Toulouse in collaboration with Tractebel Engie. This model has to consider the local behaviour of paste around reactive aggregate, in terms of both cement paste creep and partial reclosing of micro-cracks.

5. REFERENCES

[1] S. Diamond, "A review of alkali-silica reaction and expansion mechanisms," *Cement and Concrete Research,* pp. 329-346, 1975.

[2] C. Larive, Apports combinés de l'expérimentation et de la modélisation à la compréhension de l'alcali-réaction et de ses effets mécaniques, Ecole Nationale des Ponts et Chaussées, 1997.

[3] S. Multon, Evaluation expérimentale et théorique des effets mécaniques de l'alcali-réaction sur des structures modèles, Ecole Nationale des Ponts et Chaussées, 2003.

[4] R. G. Charlwood, "A review of alkali aggregate reaction in hydro plants and dams," *Hydropower and Dams,* pp. 73-80, 1994.

[5] R. Esposito and M. A. N. Hendriks, "Literature review of modelling approaches for ASR in concrete: a new perspective," *European Journal of Environmental and Civil Engineering,* 2017.

[6] E. Grimal, A. Sellier, Y. Le Pape and E. Bourdarot, "Creep, Shrinkage, and Anisotropic Damage in Alkali-Aggregate Reaction Swelling Mechanism—Part I : A Constitutive Model," *ACI Materials Journal,* vol. 105, pp. 227-235, 2008.

[7] C. F. Dunant and K. L. Scrivener, "Micro-mechanical modelling of alkali-silica-reaction-induced degradation using the AMIE framework," *Cement and Concrete Research,* vol. 40, pp. 517-525, 2010.

[8] H. W. Reinhardt, H. Özkan and O. Mielich, "Creep of concrete as influenced by the rate of expansion due to alkali-silica reaction," *Structural Concrete,* pp. 1-11, 2019.

[9] LCPC, *Recommandations pour la prévention des désordres dus à l'alcali-réaction.,* 1994.

[10] A. Makani, Influence de la nature minéralogique des granulats sur le comportement mécanique différé des bétons, INSA de Toulouse, 2011, pp. 118-122.

[11] NF P18-412, Bétons - Caractéristiques particulières des machines hydrauliques pour essais de compression (presses pour matériaux durs), AFNOR, 1981.

[12] RILEM, Recommandations RILEM CPC8, Modulus of elasticity of concrete in compression, Materials and Structures, 6(30), 507-512.

[13] P. Rivard, M. A. Bérubé, J. P. Ollivier and G. Balliby, "Decrease of pore solution alkalinity in concrete tested for alkali-silica reaction," *Materials and Structures,* no. 40, pp. 909-921, 2007.

[14] NF P18-441-16, Essais pour béton durci - Partie 16 : détermination du retrait du béton, AFNOR, 2019.

[15] I. Jawed and J. Skalny, "Effects of Alkalies on Hydration and Performance of Portland Cement," *Cement and Concrete Research,* no. 8, pp. 37-52, 1978.

[16] S. Diamond, R. S. Barneyback Jr and L. J. Struble, "On the physics and chemistry of alkali-silica reactions," *Conference On Alkali-Aggregate Reactions in Concrete,* 1981.

[17] S. Poyet, Etude de la dégradation des ouvrages en béton atteints par la réaction alcali-silice, 2003: Université de Marne-La-Vallée .

[18] NF P18-594, *Granulats - Méthodes d'essai de réactivité aux alcalis,* AFNOR, 2015.